Available online at www.sciencedirect.com

ScienceDirect

Mendeleev Commun., 2022, **32**, 492–494

Mendeleev Communications

One-step synthesis of nitrogen-doped few-layer graphene structures decorated with $Mn_{1.5}Co_{1.5}O_4$ nanoparticles for highly efficient electrocatalysis of oxygen reduction reaction

Valeriy K. Kochergin,[a,b] Roman A. Manzhos,*[a] Igor I. Khodos[c] and Alexander G. Krivenko[a]

[a] *Institute of Problems of Chemical Physics, Russian Academy of Sciences, 142432 Chernogolovka, Moscow Region, Russian Federation. E-mail: rmanzhos@icp.ac.ru*

[b] *Department of Chemistry, M. V. Lomonosov Moscow State University, 119991 Moscow, Russian Federation*

[c] *Institute of Microelectronics Technology and High Purity Materials, Russian Academy of Sciences, 142432 Chernogolovka, Moscow Region, Russian Federation*

DOI: 10.1016/j.mencom.2022.07.020

A nanocomposite consisting of nitrogen-doped few-layer graphene structures, the surface of which is decorated with nanocrystallites of $Mn_{1.5}Co_{1.5}O_4$ spinel oxide, was prepared by a single-stage method of plasma-assisted electrochemical exfoliation of graphite in a solution of 1 M $NaNO_3$ + 0.005 M $MnSO_4$ + 0.005 M $CoSO_4$ + 0.01 M melamine. The high catalytic activity of the synthesized catalyst in the oxygen reduction reaction is due to pyridine nitrogen atoms and $Mn_{1.5}Co_{1.5}O_4$ spinel nanoparticles.

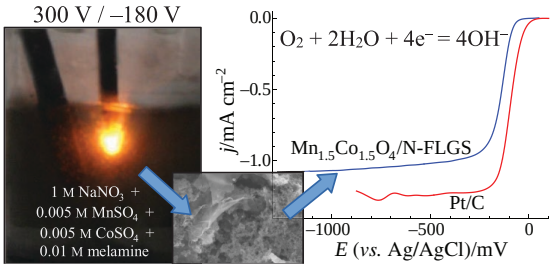

Keywords: electrochemical exfoliation of graphite, electrolytic plasma, nitrogen-doped few-layer graphene structures, $Mn_{1.5}Co_{1.5}O_4$ spinel, oxygen reduction reaction.

Since the widespread industrial introduction of noble metal catalysts in the early 20th century, numerous attempts have been made to tailor alternative catalytic materials that do not contain precious metals. This line of research received a new impetus at the end of the century in connection with the transition to green chemistry and energy, where the absence of noble metals in new materials became a prerequisite for their practical implementation. This fully applies to catalysts for the oxygen reduction reaction (ORR), which plays a key role in electrochemical energy conversion and storage devices, such as fuel cells and metal–air batteries.[1,2]

The best way to solve the problem is to design composite platinum-free ORR catalysts based on carbon nanostructures doped with p-elements, primarily N, less often S, P, B,[3–6] and decorated with transition metal oxides, such as oxides of Mn, Co, Fe and Ni.[7–9] In addition to high catalytic activity, such materials are characterized by low production costs, low toxicity and rich natural resources for their production. It has already been proposed to design composites containing carbon allotropes doped with heteroatoms, the surface of which is decorated with spinel manganese–cobalt oxides.[10–12] Despite certain difficulties in the synthesis of these composites, such electrode materials have a good potential for use as highly efficient ORR electrocatalysts.

In this communication, we report the one-step, one-pot preparation of nitrogen-doped few-layer graphene structures ($Mn_{1.5}Co_{1.5}O_4$/N-FLGS) decorated with $Mn_{1.5}Co_{1.5}O_4$ spinel oxide nanoparticles by plasma-assisted electrochemical exfoliation of graphite. This work is based on our research on plasma-electrochemical exfoliation of graphite electrodes in order to obtain platinum-free ORR catalysts.[13,14] By varying the composition of the electrolyte, it was possible to obtain a $Mn_{1.5}Co_{1.5}O_4$/N-FLGS composite material with a high catalytic activity in ORR, close to that of the commercial Pt/C catalyst.

The nanocomposite was synthesized in a solution of 1 M $NaNO_3$ + 0.005 M $MnSO_4$ + 0.005 M $CoSO_4$ + 0.01 M melamine under the action of alternating high-voltage pulses with an amplitude of +300 and –180 V, a duration of 10 ms, a rise time of 0.5 μs and a repetition frequency 8 Hz. The rather complex composition of the solution is due to the following reasons. (i) Small amounts of manganese and cobalt sulfates are required to produce Mn and Co oxides.[14,15] (ii) Preliminary experiments have shown that N-doping of few-layer graphene structures up to 1 at% N can be achieved in a sodium nitrate solution. (iii) According to published data,[16] melamine acts as a source of nitrogen for doping graphene materials, so we used it to further increase the nitrogen content in the synthesized few-layer graphene structures. Details of the experimental setup, sample preparation procedure and physicochemical processes typical of electrolytic plasma have been described elsewhere.[17,18] Reference nanocomposites containing Mn_3O_4 and Co_3O_4 (Mn_3O_4/N-FLGS and Co_3O_4/N-FLGS, respectively) were also prepared.

Figure 1(*a*) presents an X-ray diffraction (XRD) pattern of the synthesized $Mn_{1.5}Co_{1.5}O_4$/N-FLGS nanocomposite. A strong peak at 26.3° corresponds to the (002) plane of the graphite crystal (PDF card 00-056-0159) with an interplanar spacing of ~0.34 nm. This reflection is due to few-layer graphene structures formed during the plasma-assisted electrochemical exfoliation of graphite.[14] The presence of spinel $Mn_{1.5}Co_{1.5}O_4$ is confirmed by diffraction peaks at 30.1°, 30.9°, 34.9°, 36.0°, 62.5° and 63.7°, which correspond to the planes (112), (200), (103), (211),

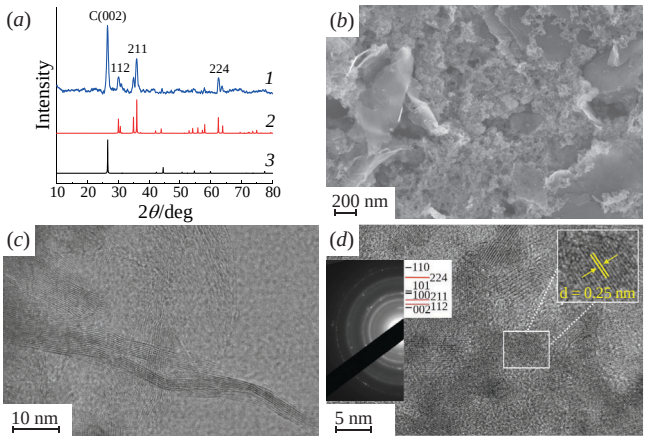

Figure 1 (*a*) XRD pattern of (*1*) the synthesized $Mn_{1.5}Co_{1.5}O_4$/N-FLGS nanocomposite and standard reference data for (*2*) $Mn_{1.5}Co_{1.5}O_4$ and (*3*) graphite from PDF cards 04-009-3194 and 00-056-0159, respectively. (*b*) SEM and (*c*),(*d*) TEM images of the $Mn_{1.5}Co_{1.5}O_4$/N-FLGS nanocomposite. The inset in (*d*) shows the corresponding SAED pattern. $Mn_{1.5}Co_{1.5}O_4$ reflections are shown as long red stripes, and graphite reflections are shown as short black stripes.

(224) and (400), respectively (PDF card 04-009-3194). The thermogravimetric analysis data shows that the amount of Mn–Co oxide has reached a value of ~50 wt% (for details, see Online Supplementary Materials). Scanning (SEM) and transmission (TEM) electron microscopy images and selected area electron diffraction (SAED) pattern of the synthesized $Mn_{1.5}Co_{1.5}O_4$/N-FLGS nanocomposite are shown in Figure 1(*b*)–(*d*). As can be seen, the material is a conglomerate of few-layer graphene sheets (FLGS), the surface of which is decorated with aggregated $Mn_{1.5}Co_{1.5}O_4$ spinel nanoparticles. The thickness of FLGS is 2–3 nm (7–10 layers of graphene), and the typical particle size of spinel Mn–Co oxide is 5–7 nm. The SAED pattern [Figure 1(*d*), inset] exhibits diffraction rings corresponding to interplanar spacings of 0.295, 0.250 and 0.150 nm in $Mn_{1.5}Co_{1.5}O_4$ spinel crystallites, consistent with XRD data.

According to X-ray photoelectron spectroscopy (XPS), the contents of O, N, Mn and Co in the surface layer of the $Mn_{1.5}Co_{1.5}O_4$/N-FLGS nanocomposite are 32.8, 5.8, 1.7 and 1.8 at%, respectively. Deconvolution of the high-resolution C 1*s* spectrum made it possible to distinguish several oxygen-containing groups (mainly carbonyl groups) on the surface of the graphene support. Deconvolution of the N 1*s* spectrum [Figure 2(*a*)] showed the presence of three peaks at 399.0, 400.5 and 401.4 eV related to the pyridine, pyrrole and graphite nitrogen atoms, contributing 2.2, 2.3 and 2.1 at% in nitrogen content in N-FLGS, respectively.[19,20] Thus, the XPS data unambiguously confirm the N-doping of graphene-like structures formed during plasma-assisted exfoliation of graphite in a melamine-containing solution. Figure 2(*b*),(*c*) shows the high-resolution spectra of Co 2*p* and Mn 2*p*, respectively. The Co 2*p* spectrum exhibits two main peaks for $2p_{3/2}$ and $2p_{1/2}$ at 780 and 795 eV, respectively, with a spin–orbit splitting of 15 eV and two satellites at 787.8 and 804.6 eV. According to generally accepted concepts,[21–23] the first component in the $2p_{3/2}$ peak at 779.9 eV can be attributed to the photoelectron response from Co^{3+} ions, while that at 781.7 eV, from Co^{2+} ions. The Mn 2*p* spectrum also exhibits two main peaks with binding energies of 640.9 eV ($2p_{3/2}$) and 652.6 eV ($2p_{1/2}$) with a spin energy separation of 11.7 eV. The spectrum can be deconvolved into four peaks, which indicate the presence of Mn^{2+} and Mn^{3+} ions.[21–23] Therefore, the above analysis confirms the co-existence of Mn^{2+}/Mn^{3+} and Co^{2+}/Co^{3+} cations in the synthesized $Mn_{1.5}Co_{1.5}O_4$/N-FLGS nanocomposite.

The catalytic activity of the synthesized catalysts in ORR was assessed on a setup with a rotating disk electrode in an air-

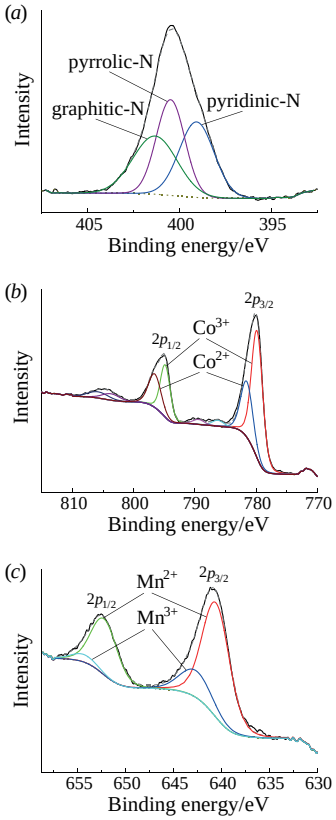

Figure 2 High-resolution (*a*) N 1*s*, (*b*) Co 2*p* and (*c*) Mn 2*p* XPS spectra of the $Mn_{1.5}Co_{1.5}O_4$/N-FLGS nanocomposite.

saturated 0.1 M KOH solution at a change in the rotation speed (ω) and the same catalyst load on glassy carbon electrodes (about 400 μg cm^{-2}). Figure 3(*a*) presents linear sweep voltammetry (LSV) curves taken at a potential scan rate (ν) of 10 mV s^{-1} for $Mn_{1.5}Co_{1.5}O_4$/N-FLGS, Mn_3O_4/N-FLGS and Co_3O_4/N-FLGS nanocomposites and, for comparison, the commercially available platinum catalyst E-TEK C1-40 (40% Pt/Vulcan XC-72, hereinafter Pt/C) at the same load. It can be seen that the performance of $Mn_{1.5}Co_{1.5}O_4$/N-FLGS is noticeably better than those of other synthesized composites, both in terms of overpotential and oxygen reduction current. For $Mn_{1.5}Co_{1.5}O_4$/N-FLGS, the half-wave potential is only 40 mV lower than for Pt/C. An analysis of the LSV curves obtained at various ω using the Koutecký–Levich equation indicated that the total number of electrons (n) participating in the ORR for $Mn_{1.5}Co_{1.5}O_4$/N-FLGS is close to 4 at $E < -200$ mV [Figure 3(*b*)]. Moreover, the high catalytic activity of the $Mn_{1.5}Co_{1.5}O_4$/N-FLGS nanocomposite is also evidenced by the slope of the Tafel plots equal to 43 mV dec^{-1} at low overpotentials.[10] In this regard, it can be stated that complete reduction of oxygen to water occurs on the $Mn_{1.5}Co_{1.5}O_4$/N-FLGS catalyst. Besides, the $Mn_{1.5}Co_{1.5}O_4$/N-FLGS nanocomposite exhibits excellent

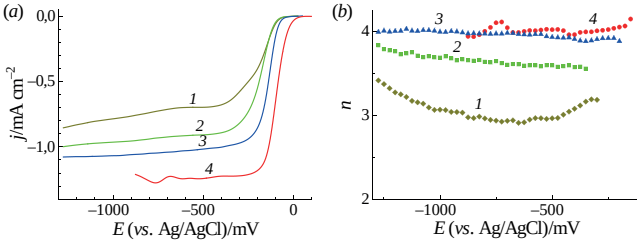

Figure 3 (*a*) LSV curves and (*b*) *n*–*E* dependences for ORR in an air-saturated 0.1 M KOH solution (ν = 10 mV s^{-1}, ω = 2000 rpm, and the current density corresponds to the geometric area of the electrode surface) on various catalysts: (*1*) Mn_3O_4/N-FLGS, (*2*) Co_3O_4/N-FLGS, (*3*) $Mn_{1.5}Co_{1.5}O_4$/N-FLGS and (*4*) Pt/C.

stability. Thus, for 5.5 h of polarization at −300 mV, the ORR current decreased by only 7%, and for the Pt/C catalyst, by 35%. In addition, an accelerated durability test showed a negative ORR overpotential shift of *ca.* 15 mV after 1000 potential cycles. The high catalytic activity observed for the $Mn_{1.5}Co_{1.5}O_4$/N-FLGS nanocomposite is due to spinel Mn–Co oxide[10] and pyridine N atoms[13,19,24] on the carbon substrate surface. Mixed-valence transition metals and defects in graphene sheets provide a large number of active sites for ORR. It is appropriate to assume that the adsorption of O_2 on Co^{2+} and Mn^{3+} ions[25] promotes oxygen reduction *via* the four-electron pathway.

Thus, for the first time, a new facile synthetic protocol for plasma-assisted exfoliation of graphite in a solution of 1 M $NaNO_3$ + 0.005 M $MnSO_4$ + 0.005 M $CoSO_4$ + 0.01 M melamine was developed to obtain a platinum-free ORR catalyst in a one-step process. The electrocatalytic activity of the synthesized $Mn_{1.5}Co_{1.5}O_4$/N-FLGS composite is not inferior to the commercial Pt/C catalyst with better long-term stability.

This work was supported by the Russian Foundation for Basic Research (project no. 19-03-00310) and performed within the framework of State Assignments nos. AAAA-A19-119061890019-5 (IPCP RAS) and 075-00355-21-00 (IMT RAS) using the equipment of the Multi-User Analytical Center of IPCP RAS and the equipment of the Multi-User Center of Scientific Center in Chernogolovka RAS. The authors are grateful to Dr. D.N. Podlesnyi (Laboratory of Technological Combustion, IPCP RAS) for carrying out the thermogravimetric analysis.

Online Supplementary Materials

Supplementary data associated with this article can be found in the online version at doi: 10.1016/j.mencom.2022.07.020.

References

1 M. Kiani, X. Q. Tian and W. Zhang, *Coord. Chem. Rev.*, 2021, **441**, 213954.
2 A. K. Worku, D. W. Ayele and N. G. Habtu, *Mater. Today Adv.*, 2021, **9**, 100116.
3 L. Qu, Y. Liu, J.-B. Baek and L. Dai, *ACS Nano*, 2010, **4**, 1321.
4 Z. Yang, Z. Yao, G. Li, G. Fang, H. Nie, Z. Liu, X. Zhou, X. Chen and S. Huang, *ACS Nano*, 2012, **6**, 205.
5 R. Li, Z. Wei, X. Gou and W. Xu, *RSC Adv.*, 2013, **3**, 9978.
6 H. Fei, R. Ye, G. Ye, Y. Gong, Z. Peng, X. Fan, E. L. G. Samuel, P. M. Ajayan and J. M. Tour, *ACS Nano*, 2014, **8**, 10837.
7 Y. Liang, Y. Li, H. Wang, J. Zhou, J. Wang, T. Regier and H. Dai, *Nat. Mater.*, 2011, **10**, 780.
8 S. Bag, K. Roy, C. S. Gopinath and C. R. Raj, *ACS Appl. Mater. Interfaces*, 2014, **6**, 2692.
9 A. Sarapuu, L. Samolberg, K. Kreek, M. Koel, L. Matisen and K. Tammeveski, *J. Electroanal. Chem.*, 2015, **746**, 9.
10 Y. Liang, H. Wang, J. Zhou, Y. Li, J. Wang, T. Regier and H. Dai, *J. Am. Chem. Soc.*, 2012, **134**, 3517.
11 A. Qaseem, F. Chen, C. Qiu, A. Mahmoudi, X. Wu, X. Wang and R. L. Johnston, *Part. Part. Syst. Charact.*, 2017, **34**, 1700097.
12 Y. Zhan, C. Xu, M. Lu, Z. Liu and J. Y. Lee, *J. Mater. Chem. A*, 2014, **2**, 16217.
13 N. S. Komarova, D. V. Konev, A. S. Kotkin, V. K. Kochergin, R. A. Manzhos and A. G. Krivenko, *Mendeleev Commun.*, 2020, **30**, 472.
14 A. S. Kotkin, V. K. Kochergin, E. N. Kabachkov, Y. M. Shulga, A. S. Lobach, R. A. Manzhos and A. G. Krivenko, *Mater. Today Energy*, 2020, **17**, 100459.
15 V. K. Kochergin, R. A. Manzhos, A. S. Kotkin and A. G. Krivenko, *High Energy Chem.*, 2020, **54**, 227 (*Khim. Vys. Energ.*, 2020, **54**, 245).
16 F. Liu, F. Niu, T. Chen, J. Han, Z. Liu, W. Yang, Y. Xu and J. Liu, *Carbon*, 2018, **134**, 316.
17 P. N. Belkin, A. Yerokhin and S. A. Kusmanov, *Surf. Coat. Technol.*, 2016, **307**, 1194.
18 A. G. Krivenko, R. A. Manzhos, A. S. Kotkin, V. K. Kochergin, N. P. Piven and A. P. Manzhos, *Instrum. Sci. Technol.*, 2019, **47**, 535.
19 L. Lai, J. R. Potts, D. Zhan, L. Wang, C. K. Poh, C. Tang, H. Gong, Z. Shen, J. Lin and R. S. Ruoff, *Energy Environ. Sci.*, 2012, **5**, 7936.
20 V. V. Chesnokov, A. S. Chichkan, D. A. Svintsitskiy, E. Yu. Gerasimov and V. N. Parmon, *Dokl. Phys. Chem.*, 2020, **495**, 159 (*Dokl. Ross. Akad. Nauk, Khim., Nauki Mater.*, 2020, **495**, 46).
21 J. F. Li, S. L. Xiong, X. W. Li and Y. T. Qian, *J. Mater. Chem.*, 2012, **22**, 23254.
22 L. Yu, L. Zhang, H. B. Wu, G. Zhang and X. W. (D.) Lou, *Energy Environ. Sci.*, 2013, **6**, 2664.
23 J. Li, S. Xiong, X. Li and Y. Qian, *J. Mater. Chem.*, 2012, **22**, 23254.
24 V. P. Vasiliev, R. A. Manzhos, A. G. Krivenko, E. N. Kabachkov and Yu. M. Shulga, *Mendeleev Commun.*, 2021, **31**, 529.
25 H. Osgood, S. V. Devaguptapu, H. Xu, J. Cho and G. Wu, *Nano Today*, 2016, **11**, 601.

Received: 19th November 2021; Com. 21/6753